

Research article

Potential of alternative waste materials: rice husk ash and waste glass cullet with boric acid addition for low-fired unglazed tiles

Purinut Maingam*, Ubolrat Wangrakdiskul and Natthakitta Piyarat

Department of Production Engineering, Faculty of Engineering, King Mongkut's University of Technology North Bangkok, Bangkok 10800, Thailand

* **Correspondence:** Email: s6201021910047@email.kmutnb.ac.th; Tel: +66924826698.

Abstract: This study aimed to investigate the potential of utilizing waste materials by adding boric acid (H_3BO_3) for producing low-fired unglazed tiles under low temperatures. Eighteen formulations containing rice husk ash (RHA), green glass cullet (GGC), and local kaolin clay (LKC) were constructed and divided into three groups with different RHA contents of 0, 10, and 20 wt%. Boric acid was also added with three amounts of 0, 2, and 3 wt% in mixtures. Specimens of these mixtures were produced by uniaxial pressing at 10 MPa and then fired at 900 °C for 1 h. The results showed that the formula of group B contained 10 wt% RHA, 60 wt% GGC, and 30 wt% LKC with the addition of 2 wt% boric acid. Moreover, the formula of group C contained 20 wt% RHA, 50 wt% GGC, and 30 wt% LKC by adding 3 wt% boric acid. Both formulas can achieve the ISO 13006 standard of ceramic tiles in terms of modulus of rupture and water absorption. Characterization of these formulas was investigated by scanning electron microscopy (SEM), X-ray diffraction (XRD), and the CIELAB colorimetric coordinates. SEM results confirmed that the glassy-phase and needle-like wollastonite crystals contributed to the development of the strength and dense microstructure of fired specimens. For XRD patterns, crystalline phases, e.g., nepheline, wollastonite-1A, and calcium silicate can improve the mechanical properties of ceramic bodies. It was concluded that reutilizing RHA and GGC wastes by adding boric acid is feasible to produce eco-friendly unglazed tiles at low sintering temperature.

Keywords: rice husk ash; green glass cullet; local kaolin clay; boric acid; low-fired unglazed tiles

1. Introduction

Currently, the global municipal solid waste (MSW) and solid wastes generation levels are of significant concern, which an estimated 2.2 and 19 billion tonnes per year of wastes by 2025 will be generated, respectively [1,2]. The abundant wastes are almost eliminated by landfilling and burning. Therefore, many entrepreneurs face the burden of high disposal costs. These problems require alternative methods to manage and alleviate for a sustainable future. Exploiting wastes is a great challenge for producing valuable products, preserving the environment, and reducing the commercial raw materials used [3].

Thailand is an agricultural country with a huge biomass alternative energy that can respond to the high energy needs. Biomass sources in Thailand can cover up to 15% of the energy demand to generate 7000 MW of electricity, as reported by Tun et al. [4]. Hence, rice husk (RH) is one of the biomass materials. It can be used as an alternative energy source to generate electricity from combustion in boilers. In the process, the burned RH was transformed to rice husk ash (RHA), a non-biodegradable waste and thus a problem for manufacturers. However, RHA generated contains a large amount of silicon dioxide or quartz (SiO_2) as a suitable silica resource in Asian countries to improve the physical properties of ceramic tiles [5]. Consequently, using RHA as a raw material in ceramic tile industries will be beneficial to the environment for further landfills reduction and disposal as well.

Nowadays, changing consumer behavior for consumer products has resulted in one-way drinking items used, i.e., glass packaging. In 2018, approximately 130 million tonnes of glass were produced, about 27 million tonnes (21%) of glass were recycled, as reported by Recovery Recycling Technology Worldwide [6]. Non-recycled waste glass degrades the environment. However, it had the potential to be used in ceramic bodies to play a role as fluxing agents (Na_2O , K_2O , and CaO) [7]. Hence, glass waste can be employed to mix in the ceramic bodies for lowering sintering temperature which can save energy and costs in the ceramic companies [8]. There are also various colors of waste glass, e.g., brown, clear, and green. However, green glass cullet (GGC) is more attractive due to its green color. This paper intends to use GGC for reducing sintering temperature, improving strength, and brightening up textures of ceramic tiles [5].

Kaolin clay was extensively used in ceramic, paint, and paper industries. It was employed as the major raw material which was found naturally occurring and mining. Due to the high content of silicon and aluminum oxide ($\text{SiO}_2\text{-Al}_2\text{O}_3$), it can also provide high strength when heated at high temperatures [9]. In this study, local kaolin clay was one of the plastic clay from Prachinburi province in Thailand. It was used to promote the strength and easy forming of specimens.

Moreover, boric acid (H_3BO_3) had been used in this study as an additive material. It is a weakly acidic white powder that is also soluble in water. When heated up above 150 °C, it loses all its water and transforms to boric oxide (B_2O_3) having a melting point of 450 °C [10]. It was one of the most important borates which can be used as a flux and binder in many industries for improving mechanical strength and reducing firing temperature, resulting in energy savings of the sintering process [11].

2. Literature review

Many studies were attempting to utilize wastes as alternative materials for producing ceramic products, focusing on the wastes of this study, e.g., RHA and glass waste. Besides, many studies had

investigated kaolin clay and boric acid for fabricating products. Thus, the previous researches can be described as follows.

The first group referred to the waste utilization of RHA. Wangrakdiskul et al. concluded that a mixture of 10 wt% RHA and 60 wt% waste glass promoted the greyish color of ceramic tiles due to the influence of RHA content after firing at 950 °C. Furthermore, it can abide by the Thai Industrial Standard (TIS 2508–2555) in terms of bending strength and water absorption [5]. Eliche-Quesada et al. proposed that the use of 10 wt% RHA and 30 wt% wood ash in clay brick fired at 1000 °C can attain the standard requirements of clay masonry units [12]. Mostari et al. indicated that 25 wt% RHA was used as quartz substitution with firing at 1050 °C and soaking for 1 h. It can promote a dense arrangement resulting in increased flexural strength of porcelain [13]. Khoo et al. reported that fired clay bricks containing 15 wt% RHA and 10 wt% sand as a replacement of clay can pass the minimum requirement for building materials after firing at 1200 °C [14]. Development of a refractory ceramic fired at 1300 °C, Sobrosa et al. showed that 10 wt% replacement of kaolin with RHA can potentially improve mechanical strength without decreasing thermal shock resistance [15]. From the above-mentioned research studies, it was concluded that RHA can be used up to 15 wt% for improving the physical properties of ceramic bodies by firing temperatures higher than 950 °C.

For utilizing waste glass, it had been used as alternative materials in ceramic products. Njindam et al. produced porcelain stoneware tiles with 30 wt% waste glass fired at 1150 °C for 2 h, mullite fibers were developed to improve the strength of specimens. It can also meet the ISO 13006 standard of ceramic tiles [16]. Wangrakdiskul indicated that wall tiles containing 60 wt% glass cullet, 30 wt% sediment soil, and 10 wt% commercial clay fired at 950 °C were able to meet the requirements of TIS 2508–2555 standard [7]. As reported about an efficient fluxing agent for reducing firing temperature of waste glass, it was described as follows. Braganca and Bergmann reported that using 25 wt% waste glass as a fluxing material for replacing feldspar in porcelain can reduce firing temperature from 1340 to 1240 °C. However, it had an effect on a slight reduction in strength, but not different for water absorption and shrinkage [17]. Moreover, tending of glass for reducing firing temperature had been reported by many studies, e.g., reducing by 10–20 °C [18], 20 °C [19], and 100 °C [8] due to its fluxing actions of Na₂O, K₂O, and CaO content of glass wastes [7].

For the reason of low-cost material, kaolin clay had been employed in this study. However, many studies had investigated the effect of using kaolin clay for producing ceramic products. Hamisi et al. suggested that the kaolin clay was a suitable firing temperature between 1300–1400 °C for 1 h due to a decrease in the porosity of ceramic tiles [20]. Menezes et al. indicated that the ceramic tiles containing up to 60 wt% of kaolin wastes resulted in low water absorption ($\approx 0.5\%$) after firing at 1150 °C. The XRD patterns also found to increase the mullite content of fired specimens [21]. Besides, some studies used local kaolin clay (LKC) from Prachinburi province in Thailand as low-cost ceramic material for promoting plasticity and easily forming specimens [5,22]. It can therefore be concluded that the use of kaolin clay provided a high strength of ceramic bodies after sintering temperature above 1150 °C.

Attempting to further about reduction firing temperature of ceramic products had been investigated. Employing potential additive, i.e., boric acid had been proposed. Hernández et al. indicated that the addition of boric acid up to 3 wt% resulted in decreased porosity due to increasing glass phase and mullite formation for clay-based ceramics after firing at 1100–1300 °C. However, the use of 5 wt% boric acid addition was not recommended due to the partial rehydration in the glassy phase which affected the decreasing of mullite content [23]. Başpınar et al. concluded that the use of

fly ash without any addition of boric acid found a very weak strength of fired bricks with firing temperature at 1000 °C. However, it was concluded that fly ash with the addition of 5 wt% boric acid can increase the compressive strength of clay bricks [24]. Uwe et al. reported that pulverised fuel ash (PFA) with 8 wt% boric acid addition exhibited high shrinkage when fired at 1130 °C for 1 h. This led to the deformation and warping of ceramics bodies [11].

For all of the above-mentioned studies, ceramic products utilizing RHA, waste glass, and kaolin clay with a firing temperature below 950 °C are a challenging work to improve physical properties. Consequently, boric acid was used to add with 0, 2, and 3 wt% in admixture for lowering firing temperature and improving physical properties of specimens in this study. Besides, the basic formula consists of RHA, GGC, and LKC, as derived from the previous study of Wangrakdiskul et al. [5].

This study aims to investigate the potential of boric acid addition (H_3BO_3) for producing low-fired unglazed tiles under low temperatures made from rice husk ash, green glass cullet, and local kaolin clay. The physical properties of specimens were evaluated and compared with ISO 13006 standard in terms of modulus of rupture and water absorption [25]. In addition, the colorimetric analysis was used to examine the colors of ceramic bodies by using CIELAB coordinates. For characterizing the microstructure of samples, it was carried out by scanning electron microscopy (SEM) and X-ray diffraction (XRD).

3. Materials and methods

3.1. Materials

Chemical analysis of raw materials used in this study was determined by X-ray fluorescence (XRF) analysis using the wavelength dispersive X-ray fluorescence (WDXRF) method, as expressed in Table 1. Rice husk ash (RHA) was obtained by burning the rice husk from the biomass power plant in Suphan Buri province, Thailand. The manufacturer was confronted with the problems for disposing this waste. However, it contains a high content of silicon dioxide (92.67%) which can be employed for producing ceramic products. Green glass cullet (GGC) was received from a recycling factory in Ayutthaya province, Thailand. It had been used as fluxing agents (Na_2O , K_2O , and CaO) for reducing firing temperature of fired specimens. Local kaolin clay (LKC) was taken from Prachinburi province, Thailand. It was used for promoting plasticity and easily forming of ceramic bodies. In addition, boric acid (H_3BO_3) was used as an additive material for improving mechanical strength and reducing firing temperature of ceramic tiles. Note that, it was undetectable with the XRF technique.

Table 1. Chemical composition of raw materials used.

Materials	Chemical compositions (%)											
	SiO ₂	Al ₂ O ₃	Fe ₂ O ₃	K ₂ O	CaO	MgO	TiO ₂	MnO	P ₂ O ₅	Na ₂ O	SO ₃	Cl
Rice husk ash (RHA)	92.67	0.56	0.54	1.96	1.18	0.78	0.03	0.13	1.5	0.07	0.34	0.16
Green glass cullet (GGC)	69.91	1.91	0.43	0.36	10.81	1.24	0.08	-	-	14.64	0.07	0.05
Local kaolin clay (LKC)	58.38	37.87	2.11	0.19	0.04	0.13	1.06	-	0.06	-	0.09	-
Boric acid (H_3BO_3)	Undetectable											

3.2. Methods

All the raw materials used in this study were dried to remove moisture in the electric oven at 200 °C. It was then ground under the dry condition with 100 rpm in a ball mill, the milling times for RHA, LKC, and GGC were fixed in 15, 30, and 180 min, respectively. Powder materials were sieved through 50 mesh (297 μm) with a sieve shaker. Eighteen formulas were classified into three groups (A, B, and C). They were divided with different RHA contents of 0, 10, and 20 wt%, respectively, as shown in Table 2. All formulas were added with boric acid 0 and 2 wt%. Besides, formulas of group C were improved by adding 3 wt% of boric acid for promoting 20 wt% RHA utilization. Homogeneous mixing with water was prepared. A sufficient amount of 10 wt% of water was sprayed on the mixture to obtain convenient consistency for pressing process. All mixtures were uniaxially pressed under 10 MPa into rectangular molds with the dimension (50 \times 70 \times 7 mm). After pressing, all specimens were dried to remove moisture at 200 °C for 2 h. Specimens were fired at a heating rate of 100 °C/h and soaking at the maximum temperature for 1 h that the firing parameters were received from Wangrakdiskul et al. [5]. However, previous work determined the maximum firing temperature at 950 °C [5], but the maximum firing temperature was reduced to 900 °C in this study. After that, they were naturally cooled down to room temperature in the electric kiln.

Table 2. Mixtures formulation of the experiment.

Group series	Formula no.	Composition (wt%)		
		Rice husk ash (RHA)	Green glass cullet (GGC)	Local kaolin clay (LKC)
Group A	A1	0	10	90
	A2	0	20	80
	A3	0	30	70
	A4	0	40	60
	A5	0	50	50
	A6	0	60	40
	A7	0	70	30
Group B	B8	10	10	80
	B9	10	20	70
	B10	10	30	60
	B11	10	40	50
	B12	10	50	40
	B13	10	60	30
Group C	C14	20	10	70
	C15	20	20	60
	C16	20	30	50
	C17	20	40	40
	C18	20	50	30

After firing process, three-points bending tests were performed for the evaluation of modulus of rupture (MOR) according to ISO 13006 standard [25]. Water absorption was measured the difference of wet weight by immersing in boiling water for 2 h and dry weight according to Archimedes method (ISO 13006 standard) [25]. Therefore, specimens were investigated properties

regarding; fluxing agent (Na_2O , K_2O , and CaO), modulus of rupture, water absorption, linear shrinkage, weight loss, and bulk density according to Archimedes' principle. Fifteen specimens were measured to determine the average value of each physical property testing. Furthermore, X-ray fluorescence (XRF) analysis was used to determine the chemical compositions in dry powdered materials using the wavelength dispersive X-ray fluorescence (WDXRF) spectrometer (Model: S8 TIGER, Bruker, Germany). Moreover, the CIELAB colorimetric coordinates of the colors of samples were measured in the range of 300–700 nm, using a UV-vis-NIR spectrophotometer (Shimadzu, UV-3600plus and MPC-603) equipped with analytical software (Shimadzu, UV3101PC color analysis). The CIE-L*a*b* colorimetric method was used, as recommended by the Commission Internationale de l'Eclairage (CIE). Additionally, the surface morphological analysis of the sputtered gold coatings samples was observed by scanning electron microscopy (SEM) with a model Hitachi SU3500 at voltage set on 2.5–10 kV for 5000 \times magnification. Finally, X-ray diffraction (XRD) was also conducted for obtaining mineralogical composition of powder samples, using a Bruker D8 diffractometer with $\text{Cu K}\alpha$ radiation at 0.01 $^\circ$ /s of scanning speed and a scan range of 2θ from 5 $^\circ$ to 80 $^\circ$.

4. Results and discussion

Investigation physical properties of eighteen formulas are classified into two groups. Table 3 shows the results of the sample mean and standard deviation (SD) of the first group without boric acid addition after firing at 900 $^\circ\text{C}$. While the second group by adding 2 wt% of boric acid has been reported in Table 4. Besides, all physical properties have a standard deviation of less than 10%. In this study, the addition of boric acid is expected for high-impact in terms of physical properties. Therefore, the addition of boric acid less than 2 wt% was not tested.

Table 3. Fluxing agent, modulus of rupture, water absorption, linear shrinkage, weight loss, and bulk density of fired specimens without boric acid addition.

		Formula no.																		
		A1-0	A2-0	A3-0	A4-0	A5-0	A6-0	A7-0	B8-0	B9-0	B10-0	B11-0	B12-0	B13-0	C14-0	C15-0	C16-0	C17-0	C18-0	
Compositions (%)		RHA	0	0	0	0	0	0	0	10	10	10	10	10	10	20	20	20	20	20
		GGC	10	20	30	40	50	60	70	10	20	30	40	50	60	10	20	30	40	50
		LKC	90	80	70	60	50	40	30	80	70	60	50	40	30	70	60	50	40	30
		H ₃ BO ₃	0	0	0	0	0	0	0	0	0	0	0	0	0	0	0	0	0	0
Physical properties	Fluxing agent (%)	Mean	2.79	5.35	7.9	10.46	13.02	15.58	18.14	3.09	5.64	8.2	10.76	13.32	15.88	3.38	5.94	8.5	11.06	13.62
	Modulus of rupture (MPa)	Mean	0.89	1.4	2.58	4.57	7.12	11.08	17.68	0.28	1.29	2.67	3.54	4.49	9.7	0.08	1.09	1.57	1.72	2.4
		SD	0.07	0.09	0.23	0.43	0.51	0.54	0.89	0.02	0.11	0.24	0.26	0.36	0.46	0	0.1	0.14	0.12	0.2
	Water absorption (%)	Mean	21.54	19.25	16.95	13.64	12.09	9.61	8.09	24.5	22.28	19.52	18.03	17.1	15.76	29.72	26.71	25.57	24.57	23.49
		SD	0.05	0.12	0.15	0.17	0.19	0.16	0.19	0.1	0.17	0.12	0.17	0.26	0.28	0.48	0.04	0.22	0.15	0.14
	Linear shrinkage (%)	Mean	0.64	0.97	1.27	1.53	1.84	2.51	3.53	0.38	0.59	1.08	1.64	2.01	2.84	0.4	0.63	0.79	1.3	1.8
		SD	0.06	0.09	0.11	0.07	0.13	0.14	0.09	0.03	0.05	0.06	0.08	0.07	0.07	0.03	0.05	0.03	0.03	0.08
	Weight loss (%)	Mean	6.28	5.73	5.44	4.52	3.8	3.36	2.61	7.06	6.61	5.66	5.35	4.67	3.91	7.98	7.49	6.93	6.06	5.28
		SD	0.27	0.2	0.07	0.06	0.06	0.06	0.04	0.12	0.13	0.16	0.03	0.03	0.05	0.21	0.04	0.05	0.08	0.05
	Bulk density (g/cm ³)	Mean	2.45	2.41	2.39	2.36	2.34	2.26	2.21	2.33	2.32	2.3	2.26	2.23	2.16	2.25	2.24	2.22	2.21	2.15
		SD	0.01	0.01	0.02	0.01	0.02	0.02	0.03	0.01	0.02	0.02	0.03	0.03	0.03	0.02	0.02	0.03	0.03	0.03

SD = standard deviation.

Table 4. Fluxing agent, modulus of rupture, water absorption, linear shrinkage, weight loss, and bulk density of fired specimens with 2 wt% boric acid addition.

		Formula no.																		
		A1-2	A2-2	A3-2	A4-2	A5-2	A6-2	A7-2	B8-2	B9-2	B10-2	B11-2	B12-2	B13-2	C14-2	C15-2	C16-2	C17-2	C18-2	
Compositions (%)		RHA	0	0	0	0	0	0	0	10	10	10	10	10	10	20	20	20	20	20
		GGC	10	20	30	40	50	60	70	10	20	30	40	50	60	10	20	30	40	50
		LKC	90	80	70	60	50	40	30	80	70	60	50	40	30	70	60	50	40	30
		H ₃ BO ₃	2	2	2	2	2	2	2	2	2	2	2	2	2	2	2	2	2	2
Physical properties	Fluxing agent (%)	Mean	2.79	5.35	7.9	10.46	13.02	15.58	18.14	3.09	5.64	8.2	10.76	13.32	15.88	3.38	5.94	8.5	11.06	13.62
		Modulus of rupture (MPa)	Mean	1.55	2.69	4.61	9.14	13.93	19.01	32.18	1.26	2.38	4.45	7.4	10.7	17.69	0.84	2.55	3.73	4.97
		SD	0.15	0.22	0.23	0.38	0.55	0.63	1.13	0.12	0.21	0.27	0.36	0.55	0.74	0.05	0.14	0.23	0.41	0.44
	Water absorption (%)	Mean	21.25	18.87	16.41	12.91	10.16	8.1	1.91	24.24	22	19.23	17.31	16.29	16.3	27.81	24.69	23.49	22.46	22.25
		SD	0.39	0.12	0.13	0.23	0.14	0.13	0.12	0.16	0.25	0.11	0.17	0.21	0.41	0.27	0.09	0.09	0.05	0.27
	Linear shrinkage (%)	Mean	0.77	1.54	1.79	2.18	2.68	3.52	6.37	0.86	1.06	1.34	1.94	2.24	2.31	0.61	0.81	0.94	1.38	1.52
		SD	0.07	0.08	0.1	0.11	0.13	0.1	0.24	0.06	0.06	0.07	0.09	0.12	0.19	0.04	0.06	0.03	0.04	0.12
	Weight loss (%)	Mean	6.17	5.6	5.28	4.34	3.59	3.14	2.34	6.96	6.49	5.51	5.18	4.49	3.72	7.9	7.38	6.79	5.9	5.11
		SD	0.13	0.08	0.09	0.13	0.07	0.1	0.05	0.1	0.1	0.14	0.09	0.07	0.1	0.15	0.11	0.18	0.1	0.05
	Bulk density (g/cm ³)	Mean	2.4	2.37	2.34	2.3	2.28	2.2	2.16	2.3	2.28	2.25	2.2	2.09	1.78	2.21	2.19	2.15	2.09	1.89
		SD	0.01	0.01	0.02	0.03	0.02	0.03	0.03	0.02	0.02	0.03	0.02	0.03	0.04	0.03	0.02	0.03	0.04	0.04

SD = standard deviation.

4.1. Modulus of rupture (MOR)

The MOR results of eighteen formulas with the addition of 0 and 2 wt% boric acid are illustrated in Tables 3 and 4, respectively. The high contents of fluxing agents (Na_2O , K_2O , and CaO) in GGC have been related to an increase in MOR of specimens [7]. Therefore, the highest MOR of formulas A7-0, B13-0, and C18-0 has the highest GGC content of each group. In contrast, reducing MOR is observed with mixing of RHA (≥ 10 wt%) in group B and group C due to the effect of reducing the fluxing agents and increasing porosity of RHA after combustion, it corresponds to Kazmi et al. [26]. For without boric acid and the addition of 2 wt% boric acid, MOR values of all formulas are within the range of 0.08–17.68 MPa and 0.84–32.18 MPa, respectively. It can be concluded that formulas A7-0, A6-2, A7-2, and B13-2 can attain the minimum requirement of the ISO 13006 standard of ceramic tiles in terms of MOR (>15 MPa) [25]. Note that, the effect of boric acid contributes to the increase in the MOR of specimens. Besides, the addition of 2 wt% of boric acid can reduce firing temperature from 950 to 900 °C (reducing by 50 °C) without affecting MOR properties of ceramic bodies as compared with the previous study of Wangrakdiskul et al. [5].

4.2. Water absorption

The results of adding 0 and 2 wt% boric acid on water absorption of all formulas are shown in Tables 3 and 4, respectively. The effect of boric acid addition can improve the melting behavior of ceramic bodies [24]. Therefore, water absorption of specimens with 2 wt% boric acid addition with the range of 1.91–27.81% is lower than that of without boric acid addition with the range of 8.09–29.72%. In addition, it can be concluded that increasing GGC content into a mixture results in less water absorption due to its fluxing action of GGC [7]. Therefore, the formulas A7-0, B13-0, and C18-0 have the highest GGC content, leading to the lowest water absorption and highest MOR of each group. When increasing RHA in groups B and C, this phenomenon of fired specimens will leave the highly porous structure resulting in high water absorption of specimens [5]. Note that, the results of reducing in water absorption have resulted in increased MOR of fired specimens with a similar conclusion of Carretero et al. [27].

4.3. Linear shrinkage, weight loss, and bulk density

The linear shrinkage of specimens increases due to the effect of promoting melting behavior with a high content of GGC and boric acid addition. However, the low content of the fluxing agents in groups B and C has affected low linear shrinkage due to the high RHA content of specimens. The combinations of 50–60 wt% GGC and 10–20 wt% RHA with 2 wt% boric addition of formulas B13-2 and C18-2 result in decreased linear shrinkage as compared with formulas B13-0 and C18-0 without boric addition. Moreover, formulas A1-0, B8-0, and C14-0 (without boric acid) have the highest weight loss with the high content of LKC. Due to having a high carbonaceous matter of LKC, it leads to a high weight loss of ceramic bodies after burning [7]. The bulk density of fired specimens decreases with increasing contents of GGC and RHA. This is the effect of the low specific gravity of these materials [28,29]. In contrast, the higher bulk density of all samples is due to the addition of LKC content [5], the only plastic material in this study. However, the addition of boric acid has practically no effect on the bulk density of fired specimens, since a slight decrease is observed in

Tables 3 and 4. Except for formulas B13-2 and C18-2 with 2 wt% boric acid addition, their mixtures of high GGC content are mixed with 10 wt% and 20 wt% RHA, respectively. They greatly contribute to low bulk density, leading to lowering linear shrinkage as compared without boric acid addition of formulas B13-0 and C18-0.

4.4. Comparison of physical properties with ISO 13006 standard

As compared of physical properties with the ISO 13006 standard in terms of MOR and water absorption of specimens [25], as shown in Table 5. Without the addition of boric acid, formula A7-0 utilizing 70 wt% GGC and 30 wt% LKC can attain the minimum MOR requirement of wall tiles class BIII (thickness < 7.5 mm). However, water absorption requirement ($6\% < E \leq 10\%$) can pass the ISO 13006 standard class BII_b with an average value of 8.09%. Therefore, as a whole, the quality of formula A7-0 should be classified in class BIII of ISO 13006 standard. Besides, the addition of 2 wt% of boric acid, formulas A6-2 and A7-2 utilizing 60–70 wt% GGC can meet floor tiles class BII_b and BI_b, respectively. Furthermore, utilizing various waste materials is the main objective of this study. Therefore, formula B13-2 utilizing 10 wt% RHA and 60 wt% GGC can achieve wall tile class BIII. However, utilizing RHA higher than 10 wt% is a further investigation.

Table 5. Comparing physical properties with ISO 13006 standard of ceramic tiles.

Formula no.	Compositions (wt%)				BI _b ; floor tiles		BII _b ; floor tiles		BIII; wall tiles	
	RHA	GGC	LKC	H ₃ BO ₃	MOR >30 MPa	Water absorption 0.5% < E ≤ 3%	MOR >18 MPa	Water absorption 6% < E ≤ 10%	MOR >15 MPa	Water absorption 10% < E ≤ 20%
A7-0	0	70	30	0	-	-	-	8.09	17.68	-
A6-2	0	60	40	2	-	-	19.01	8.10	-	-
A7-2	0	70	30	2	32.18	1.91	-	-	-	-
B13-2	10	60	30	2	-	-	-	-	17.69	16.30

4.5. Effect of increasing boric acid addition in group C (20 wt% RHA)

A high-utilizing of RHA for producing unglazed tiles is the main objective of this study. Formulas of group C utilizing 20 wt% RHA without boric acid and 2 wt% boric acid addition have been conducted. The physical properties of these groups cannot achieve the ISO 13006 standard, as depicted in Table 5. For improving the mechanical properties of ceramic bodies, adding 3 wt% boric acid in formulas of group C has been conducted, as shown in Table 6. The results indicate that the effect of adding 3 wt% boric acid can increase MOR and decrease water absorption of fired specimens. Except formula C18-3 is slightly expanded of specimens resulting in increased water absorption as compared with formulas C18-0 and C18-2. When comparing physical properties with the ISO 13006 standard, formula C18-3 has increased MOR from 8.22 to 12.36 MPa as compared to formula C18-2 with the addition of 2 wt% boric acid. It is higher than 12 MPa of MOR that can attain the minimum MOR requirement (>12 MPa) of wall tiles class BIII for thickness ≥ 7.5 mm [25]. Therefore, formula C18-3 can also achieve the ISO 13006 standard in terms of MOR [25]. However, water absorption requirement ($10\% < E \leq 20\%$) cannot pass the ISO 13006 standard with an average exceeds 20% due to increased porosity of RHA after combustion [25].

Table 6. Physical properties of group C (20 wt% RHA) by adding 3 wt% boric acid.

Formula no.	Compositions (wt%)				Physical properties									
	RHA	GGC	LKC	H ₃ BO ₃	Modulus of rupture (MPa)	SD	Water absorption (%)	SD	Linear shrinkage (%)	SD	Weight loss (%)	SD	Bulk density (g/cm ³)	SD
C14-3	20	10	70	3	1.46	0.10	26.79	0.11	0.91	0.04	7.58	0.09	2.19	0.02
C15-3	20	20	60	3	3.18	0.07	24.12	0.08	0.99	0.05	6.79	0.07	2.15	0.03
C16-3	20	30	50	3	5.16	0.26	22.94	0.13	1.28	0.03	6.22	0.10	2.07	0.03
C17-3	20	40	40	3	7.92	0.32	22.12	0.18	1.43	0.04	5.17	0.08	1.90	0.04
C18-3	20	50	30	3	12.36	0.48	24.10	0.21	0.11	0.01	4.17	0.06	1.52	0.05

SD = standard deviation.

4.6. The CIELAB colorimetric coordinates

From Tables 5 and 6, it is concluded that five formulas can pass the ISO 13006 standard by adding boric acid with three amounts of 0, 2, and 3 wt% in mixtures [25], e.g., A7-0, A6-2, A7-2, B13-2, C18-3. For classification colors of these formulas, the CIELAB colorimetric coordinates (L*, a*, and b*) of the colors of samples can be analyzed according to the CIE-L*a*b* standard colorimetric method, following L* is the lightness axis (black (0)→white (100)), a* is the green (−)→red (+) axis, and b* is the blue (−)→yellow (+) axis [30]. Colorimetric coordinates of these formulas are L* (42.25–57.6), a* (−0.64–8.33), and b* (4.39–22.98), as listed in Table 7. In addition, CIELAB graphics of unglazed tiles are shown in Figure 1a. As can be seen, the color of formula A7-2 shows a brighter because the L* value is higher than that of all colors. The a* value in negative of formulas A7-2, B13-2, and C18-3 is found, indicating the color generates the green tones in specimens. Besides, formula A7-0 is the highest the b* value of specimens, resulting in a high yellow color tone. Texture samples are also shown in Figure 1b–f.

Table 7. CIELAB color coordinates of samples.

Formula no.	Compositions (wt%)				CIELAB color coordinates		
	RHA	GGC	LKC	H ₃ BO ₃	L*	a*	b*
A7-0	0	70	30	0	57.2	8.33	22.98
A6-2	0	60	40	2	51.95	7.15	15.51
A7-2	0	70	30	2	57.6	−0.64	9.78
B13-2	10	60	30	2	47.18	−0.49	6.1
C18-3	20	50	30	3	42.25	−0.05	4.39

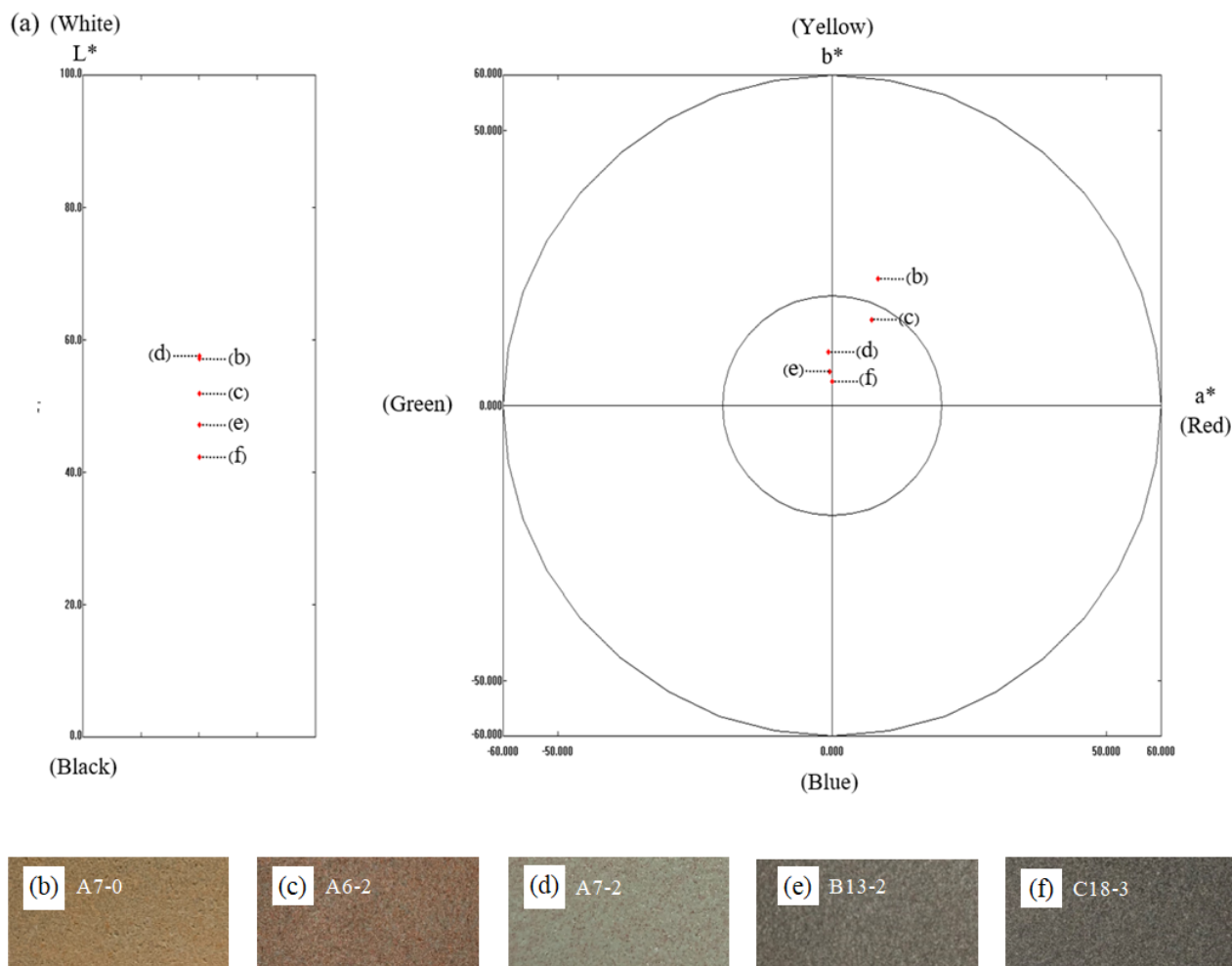


Figure 1. (a) CIELAB graphics of unglazed tiles. Texture samples: (b) formula A7-0, (c) formula A6-2, (d) formula A7-2, (e) formula B13-2 (10 wt% RHA), and (f) formula C18-3 (20 wt% RHA).

4.7. Scanning electron microscopy (SEM) analysis

SEM technique has been employed to examine the microstructure. The lowest and highest MOR of formulas A1-2 and A7-2 in group A, the highest MOR of group B (formula B13-2) and group C (formula C18-3), they have been selected to investigate the microstructure at 5000 \times magnification, as shown in Figure 2. In addition, formula A7-0 is the highest MOR of the group without boric acid that is selected to compare with formula A7-2 (the highest MOR with the addition of 2 wt% boric acid). It is found that there is the distribution of small and large-sized pores in the specimens of formula A1-2, as illustrated in Figure 2a. This leads to lowering of the MOR of specimens [5]. SEM images of the formulas A7-0, A7-2, B13-2, and C18-3 show the well-sintered body filling with the high content of fluxing oxides from GGC content, resulting in increased dense structure and glassy phase fused-bond of samples [8], as depicted in Figure 2b–e. The needle-like wollastonite crystals have also occurred in formulas A7-0, A7-2, B13-2, and C18-3 with three amounts of 0, 2, and 3 wt% boric acid and high GGC content in mixtures, as shown in Figure 2b–e.

It can improve the mechanical properties of ceramic bodies [31]. Moreover, formula A7-0 (Figure 2b) has needle-like wollastonite crystals lower than formula A7-2 (Figure 2c). Therefore, formula A7-0 has resulted in decreased MOR and increased water absorption (WA) as compared with formula A7-2.

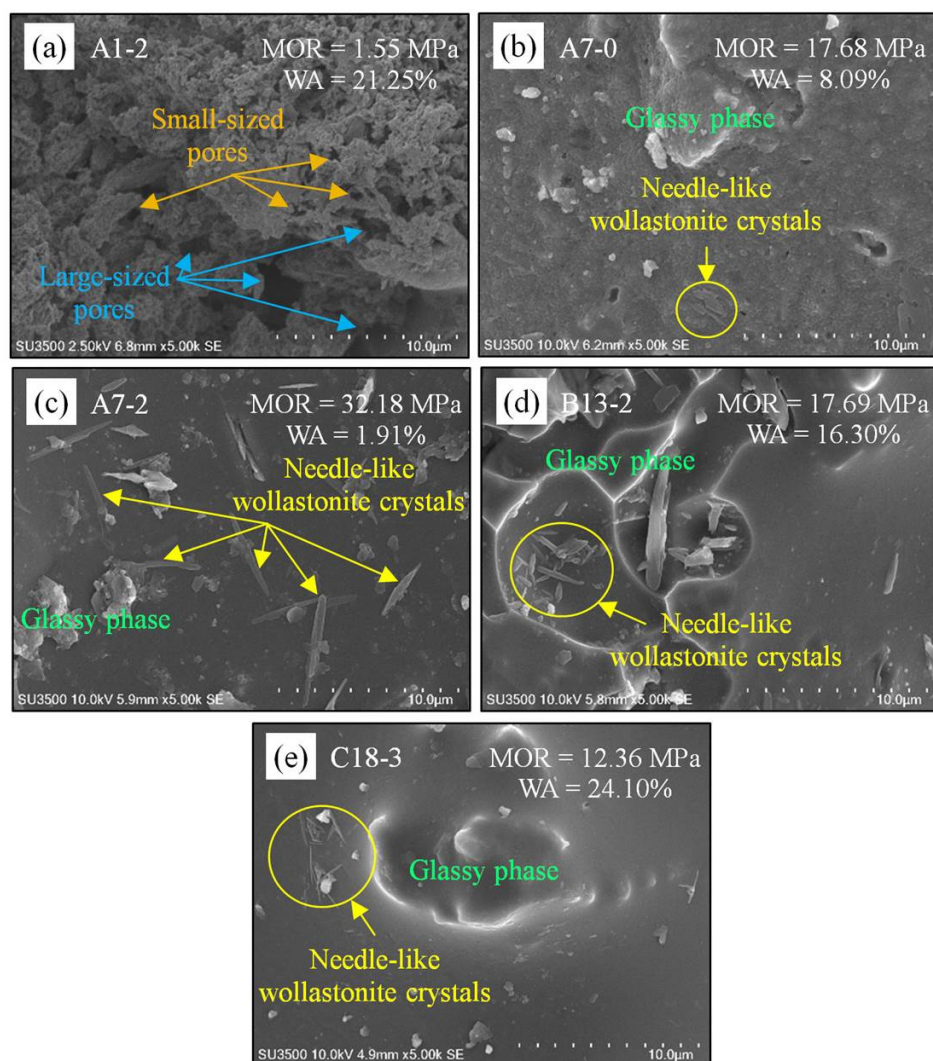


Figure 2. SEM images of structural characteristics at 5000 \times magnification of samples fired at 900 $^{\circ}$ C: (a) formula A1-2, (b) formula A7-0, (c) formula A7-2, (d) formula B13-2 (10 wt% RHA), and (e) formula C18-3 (20 wt% RHA).

4.8. X-ray diffraction (XRD) analysis

Five formulas have been examined by SEM also further investigating the mineralogical structure by XRD pattern. Crystalline phases, e.g., quartz (α -SiO₂, ICDD 01-079-1910), cristobalite low (SiO₂, ICDD 01-076-0941), nepheline (Na₃K(Al₄Si₄O₁₆), ICDD 01-076-2469), wollastonite-1A (Ca_{0.968}Mn_{0.032}SiO₃, ICDD 01-076-0528), and calcium silicate (CaSiO₃, ICDD 01-089-6463) are found in samples, as shown in Figure 3. The formula A1-2 contains quartz and cristobalite low as major crystalline phases, as depicted in Figure 3a. Without boric acid addition, formula A7-0 has mainly crystalline phases of quartz, cristobalite low, nepheline, and wollastonite-1A, as

illustrated in Figure 3b. Moreover, the mineral compositions of formulas A7-2, B13-2, and C18-3 are mainly quartz, cristobalite low, nepheline, wollastonite-1A, and calcium silicate phases, as shown in Figure 3c–e.

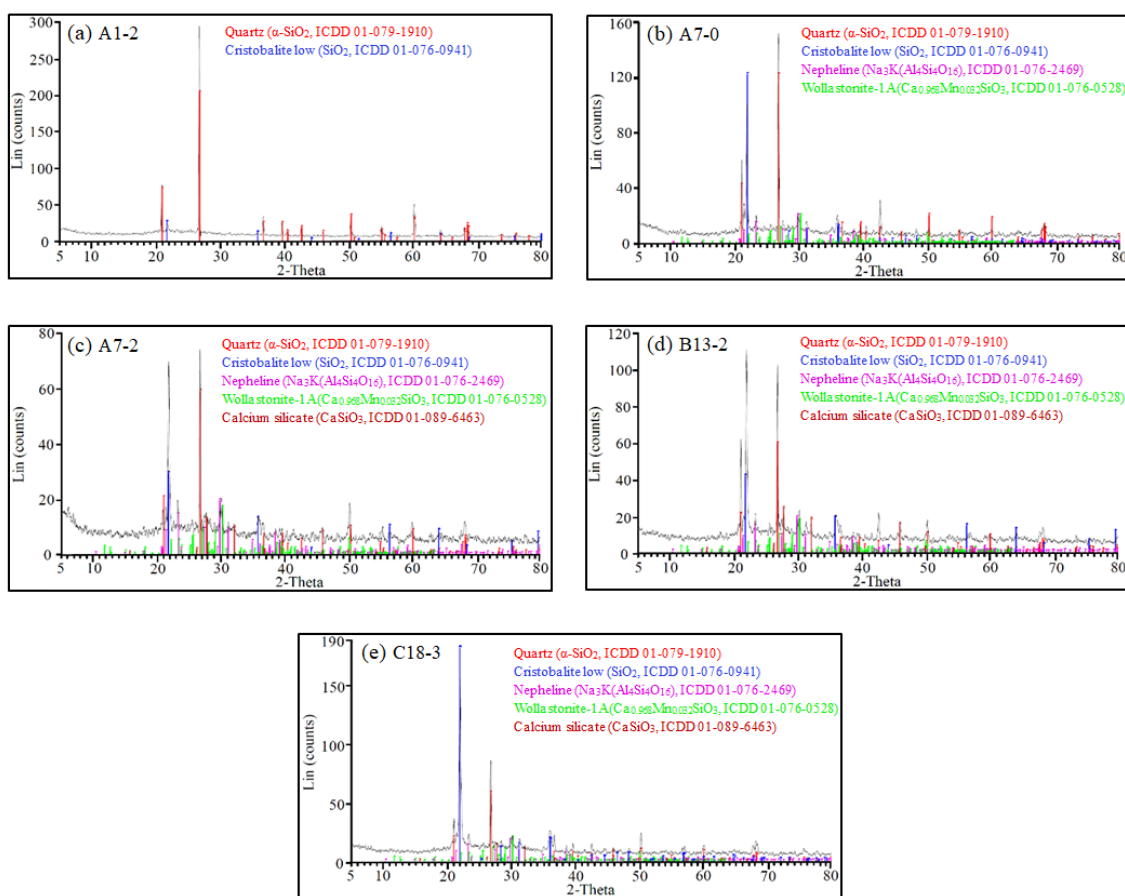


Figure 3. XRD pattern of the mineralogical composition of samples fired at 900 °C: (a) formula A1-2, (b) formula A7-0, (c) formula A7-2, (d) formula B13-2 (10 wt% RHA), and (e) formula C18-3 (20 wt% RHA).

4.8.1. For quantitative phase analysis of powder samples

The phase contents of quartz, cristobalite low, wollastonite-1A, nepheline, calcium silicate, and amorphous are investigated by TOPAS (Total Pattern Analysis Solution) software with the Rietveld method. The R_{wp} (R-weighted pattern) and GOF (goodness of fit) disagreement factors are monitored as the indicators for the refinement quality level. For all refined patterns, R_{wp} values are different from 10.55–11.78. This is an indicator for misfits between the measured and calculated data. The GOF values are within the range of 1.14–1.48. Note that, R_{wp} factor should be low values to give a good indication and the GOF value should be in the vicinity of 1 value [32]. In this study, these values are sufficient for low misfits of the observed by XRD pattern. Moreover, the main chemical compounds of samples are quartz (14.65–65.26%), cristobalite low (4.44–34.68%), nepheline (4.41–9.89%), wollastonite-1A (10.13–16.06%), calcium silicate (1.18–3.16%), and the amorphous phase (26.3–34.95%), as listed in Table 8.

Table 8. Phase quantities and Rietveld disagreement factors (R_{wp} and GOF).

No.	Compositions (wt%)				Phase quantities (%)						R_{wp}	GOF
	RHA	GGC	LKC	H ₃ BO ₃	Quartz	Cristobalite low	Nepheline	Wollastonite-1A	Calcium silicate	Amorphous		
A1-2	0	10	90	2	65.26	4.44	-	-	-	30.30	10.55	1.48
A7-0	0	70	30	0	19.93	32.54	9.89	11.34	-	26.30	11.53	1.38
A7-2	0	70	30	2	24.88	18.52	8.03	16.06	3.16	29.35	10.79	1.18
B13-2	10	60	30	2	15.97	29.61	5.94	11.81	2.58	34.09	11.78	1.14
C18-3	20	50	30	3	14.65	34.68	4.41	10.13	1.18	34.95	11.37	1.16

4.8.2. Comparison of phase quantities with MOR and water absorption properties

XRD data, MOR, and water absorption are presented in Table 9. For the addition of 2 wt% boric acid, formula A1-2 has mainly crystalline phases of quartz and cristobalite low resulting in the lowest MOR due to the high content of LKC and high porosity structure. Comparison of formulas A7-0 (without boric acid) and A7-2 (the addition of 2 wt% boric acid), the results show that formula A7-2 has higher wollastonite-1A and calcium silicate than that of formula A7-0 due to the influence of boric acid addition. It can also promote the strength of ceramic bodies, as also reported a similar effect of Obeid [33]. For considering the influence of RHA content, the crystalline contents of formulas A7-2, B13-2, and C18-3 have been compared. They indicate that nepheline, wollastonite-1A, and calcium silicate phases increase more significantly the MOR of ceramic tiles. This effect has similar results corresponding with the previous research [34–36]. Therefore, containing nepheline, wollastonite-1A, and calcium silicate phases of formula A7-2 is higher than that of formulas B13-2 and C18-3, resulting in formula A7-2 having the highest MOR and lowest water absorption. Moreover, the amorphous phase quantities of these formulas are within the range of 26.30% to 34.95%. Therefore, the amorphous phase corresponds to the bulk mineral composition of samples [37].

Table 9. Phase quantities, MOR, and water absorption.

No.	Compositions (wt%)				Phase quantities (%)						MOR (MPa)	Water absorption (%)
	RHA	GGC	LKC	H ₃ BO ₃	Quartz	Cristobalite low	Nepheline	Wollastonite-1A	Calcium silicate	Amorphous		
A1-2	0	10	90	2	65.26	4.44	-	-	-	30.30	1.55	21.25
A7-0	0	70	30	0	19.93	32.54	9.89	11.34	-	26.30	17.68	8.09
A7-2	0	70	30	2	24.88	18.52	8.03	16.06	3.16	29.35	32.18	1.91
B13-2	10	60	30	2	15.97	29.61	5.94	11.81	2.58	34.09	17.69	16.30
C18-3	20	50	30	3	14.65	34.68	4.41	10.13	1.18	34.95	12.36	24.10

5. Conclusions

Utilizing waste materials; rice husk ash (RHA), green glass cullet (GGC) mixed with local kaolin clay (LKC) and boric acid addition (H₃BO₃) for producing low-fired unglazed tiles. It is the objective of this study. From the experimental results, the following conclusions could be drawn.

- (1) Five formulas of this experiment can pass the ISO 13006 standard which can be described as follow.

- (1.1) Without the addition of boric acid, formula A7-0 utilizing 70 wt% GGC and 30 wt% LKC can attain the minimum MOR and water absorption requirements of the unglazed wall tiles class BIII. However, RHA is not utilized in this formula.
- (1.2) Adding 2 wt% boric acid without RHA content, formulas A6-2 and A7-2 utilizing 60–70 wt% GGC can fabricate the unglazed floor tiles class BII_b and BI_b, respectively. Besides, formula B13-2 containing 10 wt% RHA and 60 wt% GGC can produce the unglazed wall tiles class BIII.
- (1.3) Adding 3 wt% boric acid can be improved the physical properties in group C (20 wt% RHA), formula C18-3 can pass the unglazed wall tiles class BIII in terms of MOR. However, water absorption exceeds 20% due to increased porosity of RHA after combustion and the effect of boric acid addition.
- (2) Note that, linear shrinkage of formulas B13-2 and C18-3 decreases due to the over-firing with the effect of high boric acid addition. Both formulas have a low bulk density resulting in high water absorption, but no significant effect on the strength of specimens.
- (3) The effect of boric acid contributes to high linear shrinkage resulting in high MOR and low water absorption.
- (4) The glassy-phase and needle-like wollastonite crystals in specimens can contribute to the strength of the unglazed tiles which is confirmed by SEM analysis. For XRD patterns, crystalline phases, e.g., nepheline, wollastonite-1A, and calcium silicate can promote the mechanical properties of ceramic bodies.
- (5) The optimal addition of boric acid up to 3 wt% can reduce firing temperature from 950 to 900 °C (reducing by 50 °C) without affecting mechanical properties by confirming these results with SEM technique and XRD pattern.

As a result, a remarkable environmental and ecological achievement of reutilizing RHA and GGC wastes for manufacturing low-fired unglazed tiles can alleviate the burden of entrepreneurs by reducing the disposal cost and environmental pollution.

Acknowledgements

The authors are grateful for all necessary resources by the Production Engineering Department, Faculty of Engineering, King Mongkut's University of Technology North Bangkok (KMUTNB), Thailand.

Conflict of interest

All authors declare no conflicts of interest in this paper.

References

1. Pappu A, Saxena M, Asolekar SR (2007) Solid wastes generation in India and their recycling potential in building materials. *Build Environ* 42: 2311–2320.
2. Paliwal A, Chanakya HN (2020) Three-stage reactor design to convert MSW to methanol, In: Ghosh S, *Energy Recovery Processes from Wastes*, 1 Ed., Singapore: Springer.

3. Loryuenyong V, Panyachai T, Kaewsimork K, et al. (2009) Effects of recycled glass substitution on the physical and mechanical properties of clay bricks. *Waste Manage* 29: 2717–2721.
4. Tun MM, Juchelkova D, Win MM, et al. (2019) Biomass energy: An overview of biomass sources, energy potential, and management in Southeast Asian countries. *Resources* 8: 81.
5. Wangrakdiskul U, Maingam P, Piyarat N (2020) Eco-friendly fired clay tiles with greenish and greyish colored incorporating alternative recycled waste materials. *Key Eng Mater* 856: 376–383.
6. Harder J (2018) Glass recycling—Current market trends. Available from: https://www.recovery-worldwide.com/en/artikel/glass-recycling-current-market-trends_3248774.html.
7. Wangrakdiskul U (2020) Sustainable unglazed and low sintering temperature wall tiles by reutilizing sediment soil from the water supply treatment process and glass cullet. *Songklanakarinn J Sci Technol* 42: 1117–1124.
8. Phonphuak N, Kanyakam S, Chindaprasirt P (2016) Utilization of waste glass to enhance physical–mechanical properties of fired clay brick. *J Cleaner Prod* 112: 3057–3062.
9. Ogunro AS, Apeh FI, Nwannenna OC, et al. (2018) Recycling of waste glass as aggregate for clay used in ceramic tile production. *Am J Eng Res* 7: 272–278.
10. Sevim F, Demir F, Bilen M, et al. (2006) Kinetic analysis of thermal decomposition of boric acid from thermogravimetric data. *Korean J Chem Eng* 23: 736–740.
11. Uwe EA, Boccaccini AR, Cook SG, et al. (2007) Effect of borate addition on the sintered properties of pulverised fuel ash. *Ceram Int* 33: 993–999.
12. Eliche-Quesada D, Felipe-Sesé MA, López-Pérez JA, et al. (2017) Characterization and evaluation of rice husk ash and wood ash in sustainable clay matrix bricks. *Ceram Int* 43: 463–475.
13. Mostari M, Zaman T, Sen A, et al. (2018) Synthesis and characterization of porcelain body developed from rice husk ash. *Int J Eng Sci* 31: 25–31.
14. Khoo YC, Johari I, Ahmad ZA (2013) Influence of rice husk ash on the engineering properties of fired-clay brick. *Adv Mater Res* 795: 14–18.
15. Sobrosa FZ, Stochero NP, Marangon E, et al. (2017) Development of refractory ceramics from residual silica derived from rice husk ash. *Ceram Int* 43: 7142–7146.
16. Njindam OR, Njoya D, Mache JR, et al. (2018) Effect of glass powder on the technological properties and microstructure of clay mixture for porcelain stoneware tiles manufacture. *Constr Build Mater* 170: 512–519.
17. Braganca SR, Bergmann CP (2005) Waste glass in porcelain. *Mater Res* 8: 39–44.
18. Chidiac SE, Federico LM (2007) Effects of waste glass additions on the properties and durability of fired clay brick. *Can J Civil Eng* 34: 1458–1466.
19. Tucci A, Esposito L, Rastelli E, et al. (2004) Use of soda-lime scrap-glass as a fluxing agent in a porcelain stoneware tile mix. *J Eur Ceram Soc* 24: 83–92.
20. Hamisi H, Park SE, Choi BH, et al. (2014) Influence of firing temperature on physical properties of same clay and pugu kaolin for ceramic tiles application. *Int J Mater Sci Appl* 3: 143–146.
21. Menezes RR, Farias FF, Oliveira MF, et al. (2009) Kaolin processing waste applied in the manufacturing of ceramic tiles and mullite bodies. *Waste Manage Res* 27: 78–86.

22. Wangrakdiskul U, Loetchantharangkun W (2019) Utilizing green glass cullet, local ball clay and white clay for producing light greenish brown color wall tile. *EJEST* 2: 23–30.
23. Hernández MF, Violini MA, Serra MF, et al. (2020) Boric acid (H_3BO_3) as flux agent of clay-based ceramics, B_2O_3 effect in clay thermal behavior and resultant ceramics properties. *J Therm Anal Calorim* 139: 1717–1729.
24. Başpınar MS, Kahraman E, Görhan G, et al. (2010) Production of fired construction brick from high sulfate-containing fly ash with boric acid addition. *Waste Manage Res* 28: 4–10.
25. ISO 13006/2018, Ceramic tiles—definitions, classification, characteristics and marking. ISO International, 2018. Available from: <https://www.iso.org/standard/63406.html>.
26. Kazmi SMS, Abbas S, Munir MJ, et al. (2016) Exploratory study on the effect of waste rice husk and sugarcane bagasse ashes in burnt clay bricks. *J Build Eng* 7: 372–378.
27. Carretero MI, Dondi M, Fabbri B, et al. (2002) The influence of shaping and firing technology on ceramic properties of calcareous and non-calcareous illitic–chloritic clays. *Appl Clay Sci* 20: 301–306.
28. Habeeb GA, Mahmud HB (2010) Study on properties of rice husk ash and its use as cement replacement material. *Mater Res* 13: 185–190.
29. Matteucci F, Dondi M, Guarini G (2002) Effect of soda-lime glass on sintering and technological properties of porcelain stoneware tiles. *Ceram Int* 28: 873–880.
30. Lima NA, Alencar LD, Siu-Li M, et al. (2020) $NiWO_4$ powders prepared via polymeric precursor method for application as ceramic luminescent pigments. *J Adv Ceram* 9: 55–63.
31. Saravari O, Waipunya H, Chuayjuljit S (2014) Effects of ethylene octene copolymer and ultrafine wollastonite on the properties and morphology of polypropylene-based composites. *J Elastom Plast* 46: 175–186.
32. Tamer M (2013) Quantitative phase analysis based on Rietveld structure refinement for carbonate rocks. *J Mod Phys* 4: 1149–1157.
33. Obeid MM (2014) Crystallization of synthetic wollastonite prepared from local raw materials. *Int J Mater Chem* 4: 79–87.
34. Guo Y, Zhang Y, Huang H, et al. (2014) Novel glass ceramic foams materials based on red mud. *Ceram Int* 40: 6677–6683.
35. Azarov GM, Maiorova EV, Oborina MA, et al. (1995) Wollastonite raw materials and their applications (a review). *Glass Ceram+* 52: 237–240.
36. Teo PT, Anasyida AS, Basu P, et al. (2014) Recycling of Malaysia's electric arc furnace (EAF) slag waste into heavy-duty green ceramic tile. *Waste Manage* 34: 2697–2708.
37. Christogerou A, Lampropoulou P, Panagiotopoulos E (2021) Increase of frost resistance capacity of clay roofing tiles with boron waste addition. *Constr Build Mater* 280: 122493.



AIMS Press

© 2021 the Author(s), licensee AIMS Press. This is an open access article distributed under the terms of the Creative Commons Attribution License (<http://creativecommons.org/licenses/by/4.0>)